# A numerical study on fire endurance of wood beams exposed to three-side fire[*]

Jin ZHANG[†1], Qing-feng XU[2], Yi-xiang XU[3], Bin WANG[1], Jing-xiang SHANG[1]

(*1Key Laboratory of Concrete and Prestressed Concrete Structures of the Ministry of Education, Southeast University,*
*Nanjing 210096, China*)
(*2Shanghai Key Laboratory of New Technology Research on Engineering Structure, Shanghai Research Institute of Building Sciences,*
*Shanghai 200032, China*)
(*3Department of Civil Engineering, Strathclyde University, Glasgow G12 8QQ, UK*)
[†]E-mail: zhangjin0622@139.com
Received Jan. 18, 2012; Revision accepted Apr. 11, 2012; Crosschecked May 29, 2012

**Abstract:** To investigate the fire endurance of wood beams exposed to three-side fire, we conducted bearing capacity tests of two wood beams and experiments of five wood beams exposed to three-side fire. The finite element software ANSYS was also used to predict the fire endurance of those beams with the indirect order coupling method. It was found that the fire endurance decreases as the load level increases, and the reduction ratio tends to decrease. In the case of a certain load level, the fire endurance is improved if the section size is increased or covered by the fire protection coating. The central deformation increases as the fire duration increases, and the ratio of increase tends to rise. On another note, an increase in the density of wood leads to a rise in the fire endurance of a given beam. From the finite element method (FEM) calculation results, the fire endurance decreases as the load level increases, and the reduction ratio tends to decrease. When the load level is greater than 0.5, the fire endurance is significantly reduced, and it does not change significantly when the load level changes. Lastly, for a load level magnitude below 0.5, the fire endurance and load level are proportional to one another.

**Key words:** Three-side fire, Fire endurance, Load level, Fire prevention measures, Finite element analysis, Density of wood
**doi:**10.1631/jzus.A1200022          **Document code:** A          **CLC number:** TU366.2; TU352.5

## 1 Introduction

The fire endurance test of structural members is based on the time-temperature standard curve. The fire endurance is the fire exposure time till the member loses stability or integrity or adiathermancy. Wood beams are dominating bending members of wood structures, so fire endurances of wood beams are directly related to the fire-resistance of the whole structure.

Researchers started to investigate fire endurance of wood structures in the 1960s and formed systemic research methods in the 1970s. In the 1990s, a significant amount of work in this area was carried out, leading to important achievements. Van Zeeland *et al.* (2005) studied the impact of temperature to mechanical properties of wood columns, and gave a double line model to show the relationship between the increase of temperature and decrease of wood compressive strength through tests of mechanical properties of 17 groups pine poles. Konig (2005) developed a temperature-dependent double line model to show the relationship between the temperature and the elastic modules of wood. Firmanti *et al.* (2004) tested bearing performances of wood beams under different load levels, and found that fire

endurances, charring depths and weight losses are much related to load levels, and established a curve to show the relationship between the fire endurance and the stress level. Through the study of small-sized sequoia, Pering and Springer (1980) showed the relationship between the mass loss in the particular combustion process (the given maximum temperature at a specific burning duration) and the reduction of the tensile strength, which was consistent with the result analyzed by the energy approach. Lie (1977) summarized the fire endurance formula of wood beams exposed to three-side fire and wood columns surrounded by fire. Young and Clancy (2001) pointed out that buckling failure with decreased horizontal stiffness and increased slenderness ratio would occur for wood columns exposed to four-side fire. Park and Lee (2004) developed a new model to predict the fire growth behavior in a real compartment and to provide an alternative to the existing standard fire in terms of fire safety design. Njankouo et al. (2005) conducted experimental investigations to study charring rate of tropical hardwood species, and compared them with the results derived from Eurocode EC5-1.2 recommendation, Australian standard AS1720.4 relation and White's model, and finally proposed a new bilinear model. Babrauskas (2005) experimentally studied the charring of wood and provided guidance for interpretation of char patterns in fire investigations. Park et al. (2006) conducted that different adhesives give different connection strengths at ambient temperatures and show different strength losses at elevated temperatures. Hietaniemi (2007) presented a probabilistic simulation approach to assessment of the fire endurance of a wooden load-bearing beam in a fire. The results show explicitly the effectiveness of different fire safety measures in reducing the risk of structural failure. The two major drawbacks of biocomposites are their vulnerability to fire and very low bending strength, thus Giancaspro et al. (2009) dealt with an inorganic matrix to improve the fire resistance. They pointed out that the strength of these boards was increased by reinforcing with a very low percentage of high strength glass and carbon fibers. Moss et al. (2010) proposed an easy-to-use approach for the prediction of the fire resistance of bolted joints, based on an extension of Johansen's yield equations to fire conditions, including a model for the variation of the embedment strength with tempera-

ture. Peng et al. (2010) conducted fire-resistance tests of double shear timber connections and proposed new relationships whose analysis results show good agreement with the test results. Hugi and Weber (2012) studied information on fire resistance properties of room separation elements made of tropical wood species by investigating the fire behaviour of tropical wood species and subsequently assessing the fire resistance of elements made of this material. Frangi et al. (2011) conducted a comprehensive research project on the fire resistance of bonded timber elements to develop simplified design models for the fire resistance of bonded structural timber elements, and found that the structural behaviour of finger joints at elevated temperature is strongly influenced by the behaviour of the adhesive used for bonding and may govern the fire design of engineered wood products, such as glued laminated timber beams.

In recent years, with the restoration of forest resources and increased quantity of imported woods, scholars started to investigate fire performance of wood structures in China. Chen et al. (2002) established a mathematical model of wood's pyrolysis behavior in fire and discussed important influencing factors such as the initial density and the heat flow intensity. Yao et al. (2007) summarized the current status of fire protection for wood structures, and pointed out the importance of taking the fire prevention measures to improve the fire endurance of wood structures. Up to now, there are few related studies on the charring rate or the fire endurance except for Li et al. (2010), Xu et al. (2011a; 2011b; 2012) and Ru et al. (2011).

In conclusion, experimental studies on mechanical properties of wood structures under fire are limited and superficial in China. As a result, fire prevention design standard provisions can only refer to foreign norms. Although the remaining bearing capacities and fire endurances have been studied abroad, tree species that are commonly used differ greatly from those in China. Besides, there are some differences in forms of wood members and fire prevention measures between China and other countries.

Therefore, combined with common species and characteristics of wood components in China, studies on fire performance research will undoubtedly be able to provide theoretical bases for the fire design of wood structures. Through experimental and FEM

numerical calculation studies, this paper studied wood beams exposed to three-side fire which are commonly used in practice as research objects to study the influence of different load levels and surface fire protection measures on the fire endurance.

## 2 Fire experiment

### 2.1 Design and production of specimens

The research carried out the ultimate bearing capacity tests of two contrast wood beams and fire endurance tests of five wood beams exposed to three-side fire. Specimen specifications include 100 mm ×200 mm×4000 mm, and 150 mm×300 mm× 4000 mm (width×height×length). The span between load supports is 3.6 m, and a distance of 0.2 m is left at both ends of the length. Fire endurance tests and load tests were carried out at the same time. In other words, test beams were exposed to fire subject to constant load, which was determined by the ultimate bearing capacity of contrast beams multiplied by corresponding load level. Statistics are shown in Table 1. In the notation for the specimen, C represents

specimen exposed to three-side fire, P represents the painting fire retardant coating, and the value after P means the load level (the ratio of the applied load to ultimate bearing capacity of corresponding beams, %). For example, 150×300×4000 CP50 represents the 150 mm×300 mm×4000 mm specimen covered by the painting fire retardant coating exposed to three-side fire under the 50% load level.

### 2.2 Experimental

2.2.1 Experimental equipment

This fire experiment was conducted in the large-scale horizontal test furnace of the Key Laboratory of Concrete and Prestressed Concrete Structures of the Ministry of Education, Southeast University, China. The dimensions of the furnace are 4.0 m×1.5 m×2.5 m (length×width×height). Sides and bottom of the furnace were covered by asbestos. The top of the furnace was sealed by fire-resistant steel plate covered by asbestos.

2.2.2 Experimental materials

Douglas fir is used as a wood material. The density, moisture content, compressive strength parallel to grain, tensile strength parallel to grain and elastic modulus parallel to grain are shown in Table 2. They were obtained from material tests of small specimens at room temperature (20 °C).

The ceramic fiber needle blanket was used as the insulation material. The molybdenum wire is made of molybdenum and other high-quality metals. It was used to wrap the fire-resistant coating in order to isolate the flame. The K-type sheathed thermocouple made of nickel-chromium and nickel-silicon materials was used to measure temperature ranging from

**Table 1 Wood beams exposed to three-side fire**

| Specimen | Surface treatment | Specimen quantity |
|---|---|---|
| 100×200×4000[*] | | 1 |
| 100×200×4000 C25 | | 1 |
| 100×200×4000 C37.5 | | 1 |
| 100×200×4000 C50 | | 1 |
| 150×300×4000[*] | | 1 |
| 150×300×4000 C50 | | 1 |
| 150×300×4000 CP50 | Fire retardant coating | 1 |

[*] Contrast beam

**Table 2 Material properties of Douglas fir at room temperature (20 °C)**

| Specimen | Density (g/mm³) | Compression strength parallel to grain (MPa) | Tension strength parallel to grain (MPa) | Elastic modulus parallel to grain (MPa) |
|---|---|---|---|---|
| 100×200×4000[*] | 0.68 | 44.1 | 116.7 | 15 762 |
| 100×200×4000 C25 | 0.69 | 54.3 | 111.9 | 13 124 |
| 100×200×4000 C37.5 | 0.60 | 39.2 | 98.1 | 16 918 |
| 100×200×4000 C50 | 0.49 | 33.7 | 112.3 | 13 713 |
| 150×300×4000[*] | 0.61 | 33.7 | 89.2 | 12 947 |
| 150×300×4000 C50 | 0.52 | 32.4 | 111.1 | 10 155 |
| 150×300×4000 CP50 | 0.48 | 33.0 | 80.6 | 10 850 |

[*] Contrast beam

−200 to 1300 °C. The B60-2 expanding fire protection coating for wood structure of Ball Shield brand was adopted in the test.

### 2.2.3 Experiment temperature

The heating curve of the wood fire experiment is in accordance with the ISO 834 standard fire curve suggested by the International Standards Organization (1990).

### 2.2.4 Loading devices

Test beams were seated on the furnace wall. The top surface of the specimen was unexposed with the fire-resistant coating laid on the top surface. The reaction frame on the horizontal furnace platform was used to impose load to the test beams. Attention should be paid to sealing the furnace, and preventing the fire overflowing from the sides of beams. Loading

and measuring devices including the measurement of mid-span deflection of the beam are shown in Fig. 1.

Note that all scaffolds used to support displacement meters were set separately. In order to avoid the possible risk of the flame coming out from the gap between the cover and the test beam due to the big mid-span deflection in final stage of the test, the measurement of mid-span deflection (the displacement meter 2#) was placed higher over the specimen and connected by the molybdenum wire which could endure high temperatures. Displacement meters were set in the mid-span of the beam, and the data were dynamically collected by the control system of the test furnace.

The temperature of the wood beam can be obtained by thermocouples laid at different depths of the beam. The positions of thermocouples in the beam are shown in Fig. 2.
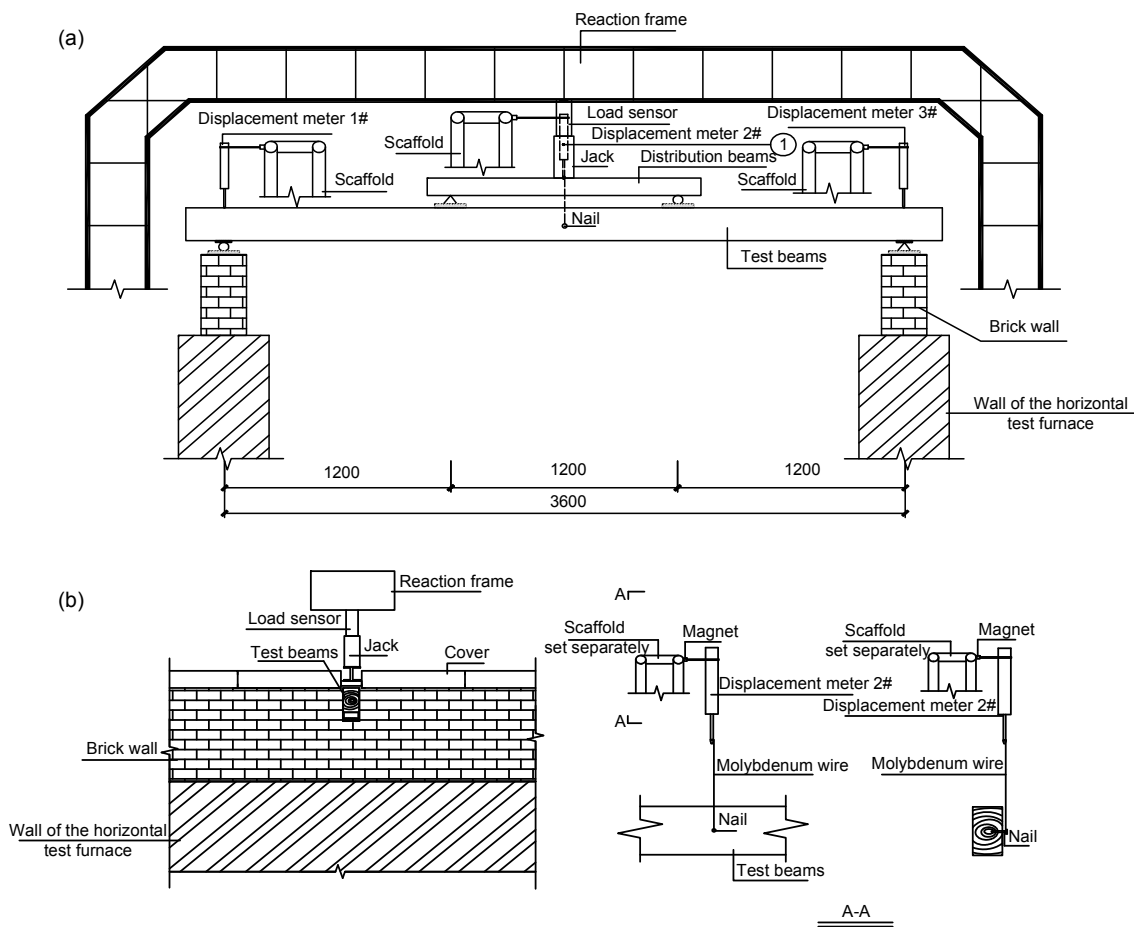


**Fig. 1  Loading and measuring devices (unit: mm)**
(a) Facade elevation; (b) Side elevation
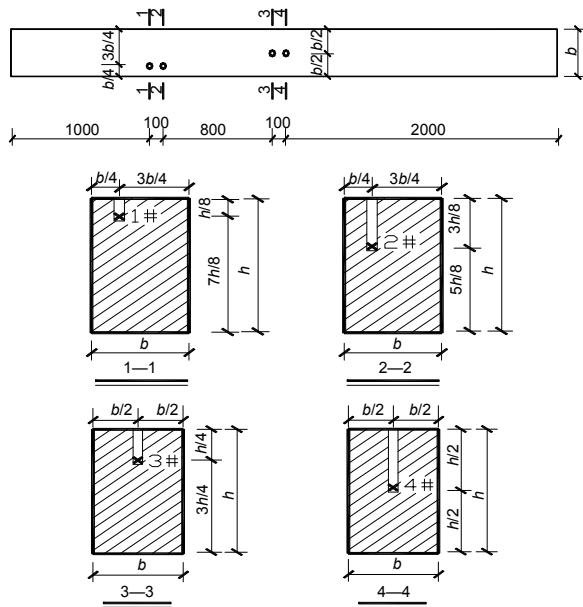
**Fig. 2  Positions of thermocouples in the beam (unit: mm)**

## 2.3  Load control

The pre-loads of 100×200×4000 group are 25%, 37.5%, 50% of the ultimate capacity of the corresponding comparing wood beam, while the pre-loads of 150×300×4000 group are 50% of the ultimate capacity of the corresponding wood beam.

The ultimate capacity of two comparing wood beams, whose sizes are 100 mm×200 mm×4000 mm and 150 mm×300 mm×4000 mm, are 33 kN and 74 kN, respectively. Thus, pre-loads of wood beams in the fire endurance test were calculated as shown in Table 3.

**Table 3  Pre-loads of wood beams in fire tests**

| Specimen | Load (kN) |
| --- | --- |
| 100×200×4000 C25 | 8.25 |
| 100×200×4000 C37.5 | 12.375 |
| 100×200×4000 C50 | 16.5 |
| 150×300×4000 C50 | 37.3 |
| 150×300×4000 CP50 | 37.3 |

The hydraulic jack was used to apply the pre-load to the desired value at a chosen speed before the fire test. The sensor was installed between the jack and the distribution beam to measure the load. The oil pressure of the hydraulic pump was manually controlled to keep the oil pressure maintained at the designed value before it was no longer constant. At this time the specimen was damaged and the fire endurance test was over.

## 2.4  Analysis of fire endurances

### 2.4.1  Criteria of the fire endurance

There are three criteria for the performances of the fire endurance: the ultimate capacity, the integrity and the insulation. Deformation and deformation rate are parameters to determine whether components have reached their ultimate capacities, and research objects are load-bearing beams. Thus, the ultimate capacity is taken as the criterion to determine the fire endurance.

For bending components, it is considered to have lost the bearing capacity when the mid-span deflection has reached $L^2/(400d)$ (mm) or the deflection rate of mid-span is greater than $L^2/(9000d)$ (mm/min), where $L$ is the span of the components, and $d$ is the height of the beam. For the specimen group 100×200×4000 ($L$=3600 mm), $L^2/(400d)$=162 mm, and $L^2/(9000d)$=7.2 mm/min. For the specimen group 150×300×4000 ($L$=3600 mm), $L^2/(400d)$=108 mm, and $L^2/(9000d)$=4.8 mm/min.

### 2.4.2  Fire endurances of wood beams

The partial specimen 150×300×4000 CP50 before fire is shown in Fig. 3a, and the failure mode of specimen 100×200×4000 C37.5 is shown in Fig. 3b. There was a rupture in the tension zone at the three-division points and the specimen was torn along the neutral axis.

Unfortunately, other specimens were all burnt into charcoal because the ultimate mid-span deflections were generally large enough to break through the enclosure and there were no other active fire extinguishing methods.

Curves of the mid-span deflection were obtained by the displacement data collected by the control system of the test furnace as shown in Fig. 4 and Fig. 5. It is shown that the deflection of the mid-span increases with the time and the ratio of increase are higher in fire. Besides, displacements undergo great changes when test beams are damaged. When a big change of displacements occurs, deflection rates are greater than the one set by the fire-endurance criteria mentioned above, and the corresponding times are fire endurances of test beams as shown in Table 4 and Fig. 6.

**Fig. 3  Photos of specimens**
(a) Specimen 150×300×4000 CP50 before fire; (b) Specimen 100×200×4000 C37.5 after fire
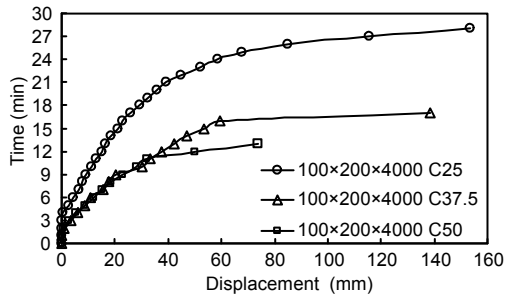


**Fig. 4  Mid-span deflection of specimen group of 100×200 ×4000**
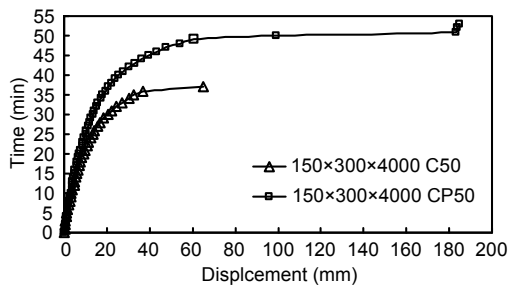


**Fig. 5  Mid-span deflection of specimen group of 150×300 ×4000**

In Fig. 6, 100 and 150 denote that the cross-sections are 100 mm×200 mm and 150 mm×300 mm, respectively. It can be seen from the left part of Fig. 6 that the fire endurance of beams with the same

cross-section size decreases as the load level increases. When the load level increases from 25% to 37.5%, the fire endurance decreases from 28 min to 17 min; when the load level increases from 37.5% to 50%, the fire endurance decreases from 17 min to 13 min. The reduction ratio decreases as the load level increases.

**Table 4  Fire endurances of wood beams**

| Specimen | Fire endurance (min) | Deflection (mm) | Deflection rate (mm/min) |
|---|---|---|---|
| 100×200×4000 C25 | 28 | 155 | 38 |
| 100×200×4000 C37.5 | 17 | 139 | 79 |
| 100×200×4000 C50 | 13 | 75 | 24 |
| 150×300×4000 C50 | 37 | 65 | 28 |
| 150×300×4000 CP50 | 51 | 183 | 84 |
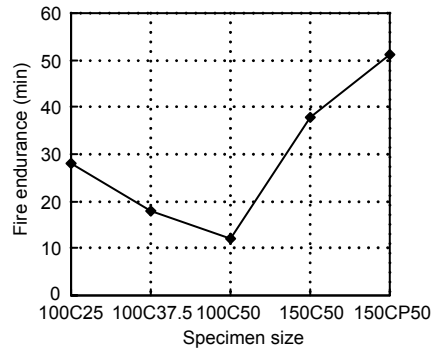


**Fig. 6  Fire endurance contrastive chart of wood beams exposed to three-side fire**

The right part of Fig. 6 shows that the fire endurance under the 50% load level increases 184% as the cross-section size increases 125%. So the increase of cross-section size is an efficient method to improve the fire endurance of wood beam exposed to three-side fire. The fire endurance can be improved about 38% by applying the fire protection coating.

In the fire test, the main variable parameters are the size of the cross-section and the load level except for the density. Although the density of each specimen is not the same, relations between test fire endurances results and densities are not clear enough due to influences of other main variable parameters mentioned above.

**2.5  Temperature changes in cross-sections**

Temperatures at different depths obtained from thermocouples are shown in Fig. 7. Furnace
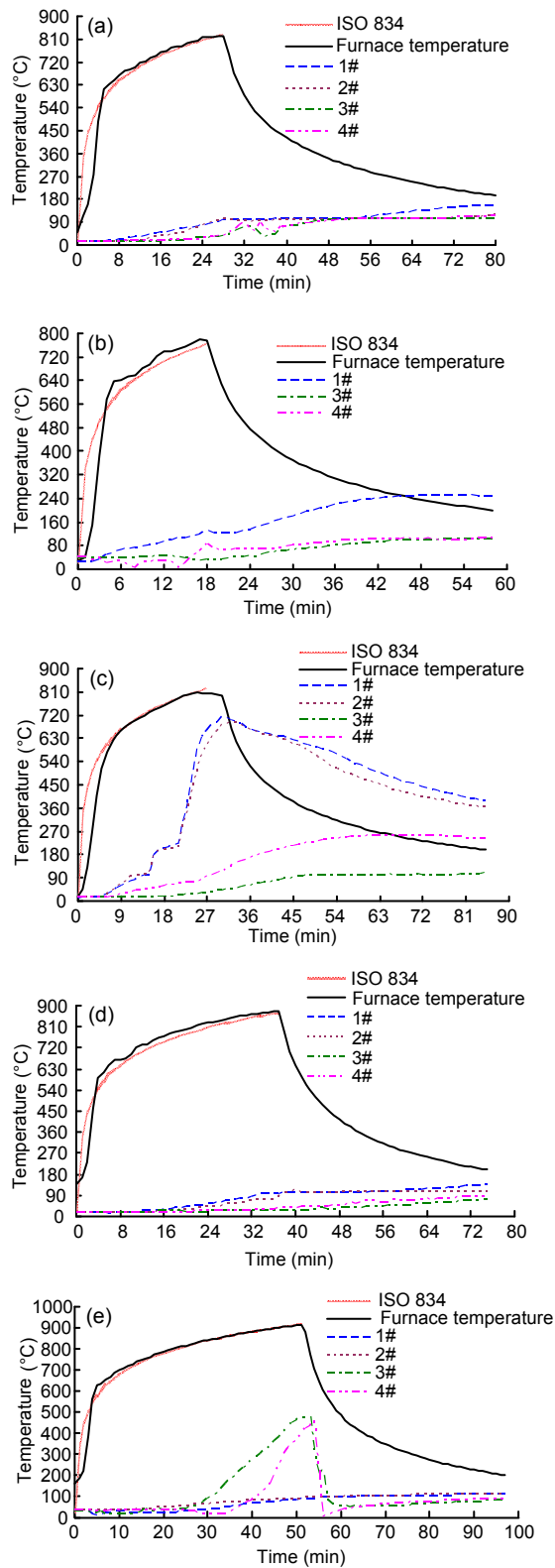
**Fig. 7  Temperatures at different depths**
(a) 100×200×4000 C25; (b) 100×200×4000 C37.5; (c) 100× 200×4000 C50; (d) 150×300×4000 C50; (e) 150×300×4000 CP50

temperature curves are in good agreement with the ISO 834 standard temperature curve. Note that the measured temperature curves of the furnace rather than the ISO 834 standard temperature curve were adopted in the following numerical study. According to temperature curves of 100×200×4000 C25, 100×200×4000 C37.5 and 100×200×4000 C50 specimens, temperature rises faster as the load level increases.

By comparing temperature curves of 150×300 ×4000 C50 with 150×300×4000 CP50 specimens, it can be seen that the interior heating rate of the test beam with fire protection coating is obviously lower than that of the corresponding test beam without fire protection coating in the beginning stage of the fire test. About 30 min later, temperatures of some measure positions increase rapidly. The reason, perhaps, is the new crack near these measurement positions.

# 3  Numerical study on fire endurance

The finite element software ANSYS is used to calculate fire endurances of wood beams exposed to three-side fire. The interaction between temperature field and structural field must be taken into consideration. The indirect order coupling method is used (Ye and Shi, 2003). First, the temperature field is obtained by thermal analysis of components. Then the temperature field considered is applied to the structural field as the body load to obtain the structural response.

## 3.1  Thermal performance of wood

The temperature distribution of the component is determined by thermal parameters of the material and boundary conditions. Thermal parameters include the heat transfer coefficient, thermal conductivity, density, specific heat capacity, etc. Also, the effect of moisture content of wood is considered in the thermal conductivity and the density.

### 3.1.1  Heat transfer coefficient

It is known from the test condition that the heat is transferred between the outside and inside of test beams by heat transfer and thermal radiation, which is the third type of the boundary condition. The heat

transfer coefficient contains the convection coefficient and the thermal radiation rate. The convection coefficient between the wood and air and the thermal radiation rate of wood in fire given by the European standard EN 1991-1-2 (2003) were used in this study. EN1991-1-2 (2003) proposes that heat convection coefficient corresponding to the ISO 834 standard heating curves is 25 W/(m$^2$·°C), and radiation ratios of the flame and wood are 1 and 0.8, respectively.

### 3.1.2 Thermal conductivity

The thermal conductivity of wood keeps changing in the process of fire. European standard EN 1991-1-2 (2003) has given the relationships between thermal conductivity and temperature as shown in Table 5. The thermal conductivity in Table 5 has taken into account the combined effect of wood and charcoal. The thermal conductivity of the carbonized layer adopts the apparent value considering the effects of cracks and carbonized consumption, rather than measurements of the thermal conductivity.

**Table 5 Thermal conductivity changing with temperature**

| Temperature (°C) | Thermal conductivity (W/(m·°C)) | Temperature (°C) | Thermal conductivity (W/(m·°C)) |
|---|---|---|---|
| 20 | 0.12 | 500 | 0.09 |
| 200 | 0.15 | 800 | 0.35 |
| 350 | 0.07 | 1200 | 1.50 |

### 3.1.3 Density

The material analyzed by the finite element software is Douglas fir. Its density has an important influence on the thermal conductivity. The change of the density is divided into five main stages for heated wood. There is little change in wood density before 100 °C. The density decreases because of evaporation of moisture when the temperature is between 100 °C and 200 °C, and reduces further because of the pyrolysis and carbonization of wood between 200 °C and 400 °C. It changes very little when the temperature is between 400 °C and 800 °C, and tends to zero and becomes negligible when the temperature is greater than 800 °C because charcoal begins to be consumed and turns into ashes eventually. Different species have different densities. Thus, the variation of density is represented by the relationship between the

density ratio (the ratio of wood density to the dry density) and the temperature as shown in Table 6, where $w$ represents the moisture content of wood.

**Table 6 Specific heat and density ratio changing with temperature**

| Temperature (°C) | Specific heat (J/(kg·°C)) | Density ratio |
|---|---|---|
| 20 | 1530 | 1+$w$ |
| 99 | 1770 | 1+$w$ |
| 100 | 13600 | 1+$w$ |
| 120 | 13500 | 1 |
| 121 | 2120 | 1 |
| 200 | 2000 | 1 |
| 250 | 1620 | 0.93 |
| 300 | 710 | 0.76 |
| 350 | 850 | 0.52 |
| 400 | 1000 | 0.38 |
| 600 | 1400 | 0.28 |
| 800 | 1650 | 0.26 |
| 1200 | 1650 | 0 |

### 3.1.4 Specific heat capacity

The amount of heat that is needed to raise the temperature (or decrease the temperature) of a unit mass of material by 1 °C is called the specific heat capacity, J/(kg·°C), and is called "specific heat" in short. The calculation formula is $C=Q/(m\cdot\Delta T)$, where $\Delta T$ is the time of endothermic or exothermic, $Q$ is the total absorbed or released heat of the object, and $m$ is the mass. The specific heat capacity of wood changing with the temperature is shown in Table 6.

## 3.2 Mechanical properties of wood under high temperature

Structural responses in fire depend on mechanical properties of wood under high temperature. The relation between strength of Douglas fir and temperature are not tested in this study. At present, related research exercises are already relatively mature and have been examined. Mechanical properties of wood keep changing with the rise of the temperature (Young and Clancy, 2001; Van Zeeland et al., 2005). Konig (2005) put forward the double line model which has been adopted by the European standard EN 1991-1-2 (2003) to show the relationships between temperature and mechanical properties such as the strength and the elastic modulus of wood as shown in Fig. 8.

In Fig. 8, note that the starting point of the curve is set at 20 °C and all relative mechanical properties are 1. The terminal point is set at 300 °C and all relative mechanical properties are 0, and the wood has already been carbonized at this point. The model of material properties is a double line one and the corresponding temperature of the turning point is 100 °C. Water in wood begins to evaporate and moisture content of wood begins to decrease at this point. European standard EN 1991-1-2 (2003) puts forward that the strength of the cork and elastic modulus should be multiplied by the corresponding reduction coefficient as the actual values. In addition, the reduction coefficient of the compression strength vertical to grain is the same as the reduction coefficient of the compression strength parallel to grain.
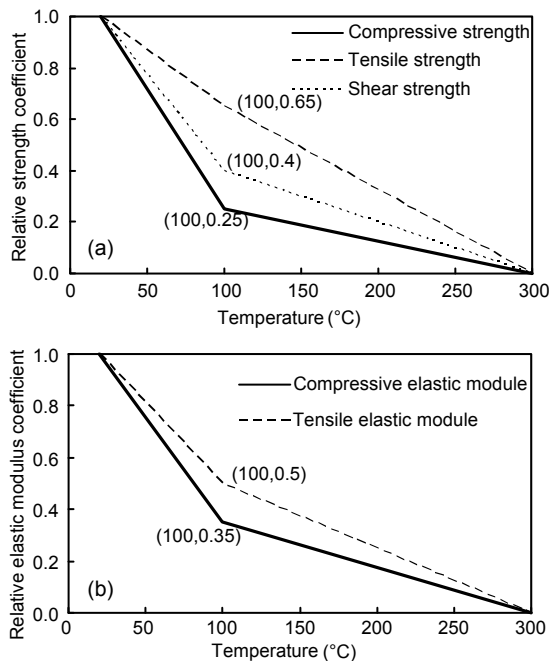


**Fig. 8 Relationship between mechanical properties and temperature (Konig, 2005)**
(a) Relative strength coefficients; (b) Relative elastic modulus coefficients

The material data at different temperatures in the fire endurance numerical study are discounted according to the double line model and the material data at 20 °C is shown in Table 2 mentioned above.

### 3.3 Finite element analysis approach

This study uses the manual method to make the thermal field coupled with the structural field in order.

The impact of the temperature field on wood properties is considered, but the impact of deformation and cracks produced in fire on temperature field is omitted.

Cracks or gaps in wood beams lead to higher heat fluxes and better ventilation. As a result, interior temperatures rise faster and charring rates increase. Richardson and Batista (2001) tested plain-edge floors made up of 38-mm thick Douglas fir decking boards in an ASTM E 119 furnace and found that the time for flame-through depends greatly on the gap between the boards. For 38 mm boards with 0 mm gap the charring rate is 1.56 mm/min. For the same specimens with 1 mm gap and 2 mm gap, charring rates increase to 2.9 mm/min and 8.4 mm/min, respectively. In the meantime, loading capacities decrease faster and fire endurances become shorter.

Ignoring cracks in the FEM analysis results in longer calculated fire endurances than the test values. Cracks in wood beams should be local. Thus, the increase of charring rates should not be as significant as that in (Richardson and Batista, 2001). Current related research is limited. Based on more data in further research combined with grading according to the status of cracks, these errors can be corrected quantitatively.

The thermal analysis uses the same model as the structural analysis in the finite element calculation. As a result, they have the same node numbers. The thermal model is converted into the structural model automatically when the thermal analysis is over. The solid 70 element, which is a type of 3D and 8-node hexahedral thermal analysis element, is used in the thermal analysis and each node has one temperature degree of freedom. The solid 70 element can be used to deal with the problem on 3D steady state or transient thermal analysis and can be replaced by an equivalent type of element such as the solid 45 element, which is also a type of 3D and 8-node hexahedral structural analysis element and used in the structural analysis.

### 3.4 Numerical calculation results of fire endurance tests

#### 3.4.1 Temperature field

Taking specimen 100×200×4000 C25 as the example, the solid 70 element is used to simulate the beams and the heat radiating element SURF152 is used to simulate heat radiating surface. In order to

reach good convergence rate only the wood beam subjected to fire (the beam between two supports) is modeled. Tetrahedral elements are used to mesh the model to take into account the carbonized layer of wood beams in fire. Numerical calculation results of the temperature distributions are shown in Fig. 9 and Fig. 10.
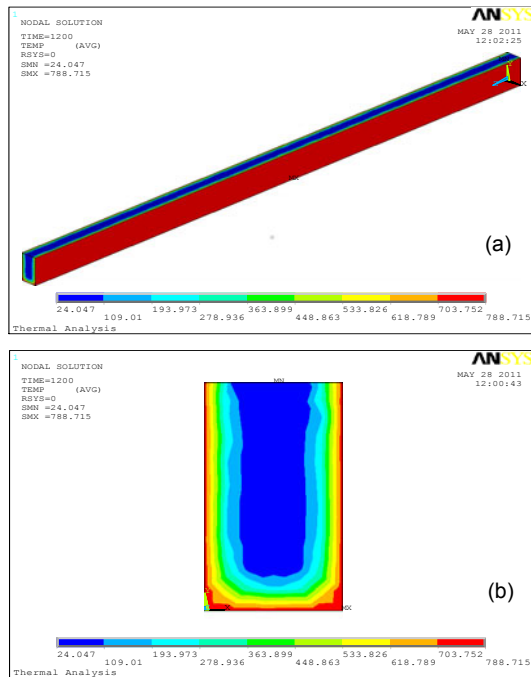


**Fig. 9  Temperature distribution of the wood beam put in fire for 20 min**
(a) Axonometric view; (b) Cross-section view
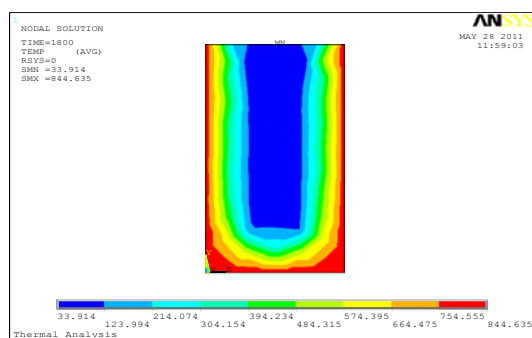


**Fig. 10  Temperature distribution of the wood beam put in fire for 30 min**

In Figs. 9 and 10, the temperature distributions of cross-sections along the length direction are the same because it is assumed that the temperature in the furnace is uniform and controlled by the ISO 834 standard heating curve. Because the corners of the beams are affected by thermal loads from two adja-

cent sides, the temperature of corners is higher and isothermal distributions of cross-section turn into a U-shape. The temperature of the bottom is higher than that of other sides at the same depth mainly because the width is smaller than the height. Temperature distribution at the bottom is affected by other sides, while the bottom temperature distribution has almost no effect on other sides. These phenomena agree with the fact that the charring rate of beam bottom is greater than that of other sides in the test.

Fig. 11 gives comparisons between FEM calculation results and test results of temperatures at 1#, 2#,
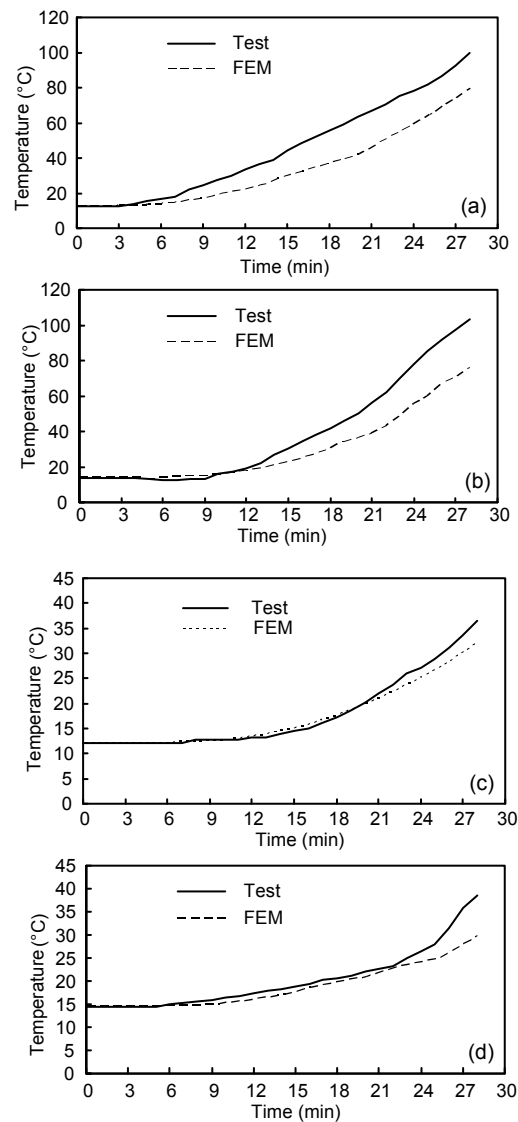


**Fig. 11  Comparisons between measured temperature and calculated temperature of specimen 100×200×4000 C25**
(a) 1# measure position; (b) 2# measure position; (c) 3# measure position; (d) 4# measure position

3# and 4# measure positions. Calculation results of 3# and 4# measure positions, 50 mm away from the edge, are matched perfectly with test values. Test values at 1# and 2# measure positions, 25 mm away from the edge, are greater than calculation results. This is possibly because that new cracks generated in test accelerated the charring rate, which was not considered in FEM. The further it is away from fire side, the closer FEM calculation results match test results. The shorter the fire duration time is, the closer the FEM results match test results.

### 3.4.2 Structural field

The solid 45 anisotropic plastic element is used to set the structural model. While modeling, $X$ axis of the global coordinate system stood for the tangential direction ($T$), $Y$ axis for the radial direction ($R$), and $Z$ axis for the longitudinal direction ($L$).

Different strengths of different regions of the test beam measured by the nailing machine were adopted in modeling. Relationships between strengths of the wood beams ($y$) and the depth ($x$) obtained from the penetrometer were fitted by a cubic curve. The relationship between the compression strength and the depth is $y=0.0002x^3+0.2593x^2-7.8688x+89.516$, and the relationship between tensile strength and the depth is $y=0.1759x^3-4.7627x^2+34.112x+44.031$. When the temperature is between 20 °C and 300 °C, material properties are discounted according to Fig. 8. When the temperature is greater than 300 °C, material properties are multiplied by a small reduction factor $10^{-6}$.

Calculation results are shown in Fig. 12. Calculation results of different times in fire, relative to the stage prior to fire with specific load level, are shown in Table 7. It is shown in Fig. 12d and Table 7 that the displacement at the mid-span of the beam increases as the time in fire increases, and the ratio of increase becomes faster.

The predicted fire endurance is 33 min, while the experimental value is 28 min, which is 18% smaller than the calculated value. The predicted ultimate mid-span deflection is 93 mm, while the experimental value is 117 mm, 26% greater than the calculation value. The discrepancy can be due to the fact that influences of structural field calculation results on the temperature field are not considered in the FEM. But in the actual test, defects of wood beams (such as cracks) accelerated the charring rate, which made the

fire endurance reduced and the mid-span deflection increased.

There are many regions where strains are not continuous in the surface of the beam. This is because the carbonization layer was simulated by material data multiplied by a reduction factor $10^{-6}$ and made strains of carbonization layer near the surface discontinuous. However, it does not affect calculation strain results of normal regions.
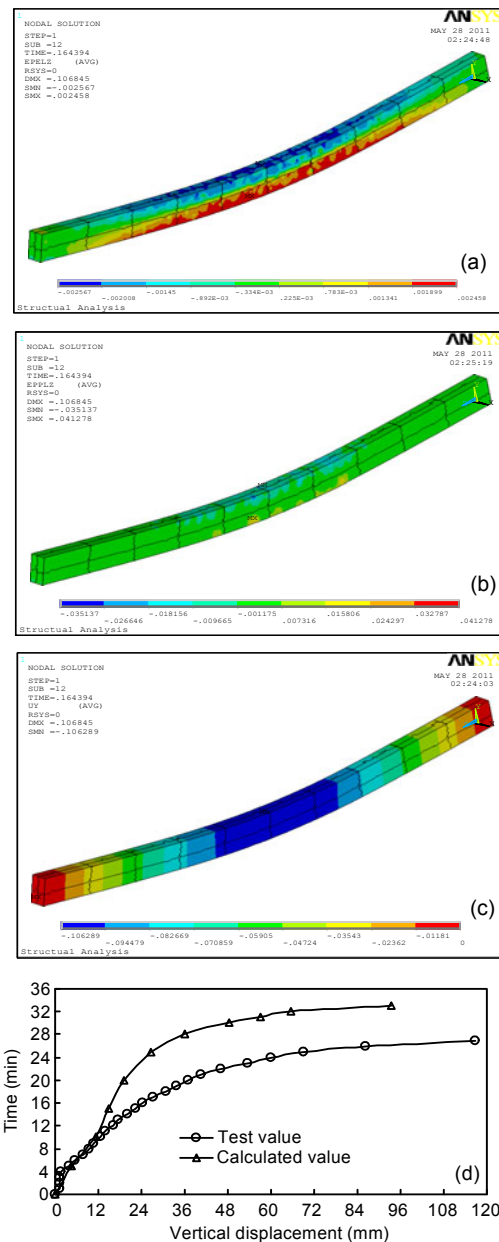


**Fig. 12  Calculation results of the 100×200×4000 C25 (the unit is meter in Figs. 12a–12c)**
(a) Elastic strains parallel to grain; (b) Plastic strains parallel to grain; (c) Vertical displacements; (d) Time-displacement curves

**Table 7 Calculation results of the 100×200×4000 C25 specimen**

| Time (min) | Vertical displacement (mm)* | Elastic strain (με) | | Plastic strain (με) | |
|---|---|---|---|---|---|
| | | $\varepsilon_{et}$ | $\varepsilon_{ec}$ | $\varepsilon_{pt}$ | $\varepsilon_{pc}$ |
| 0 | 13 | 913 | −941 | 0 | 0 |
| 5 | 17.6 | 1198 | −1200 | 9 | −9 |
| 10 | 24.25 | 1615 | −1739 | 166 | −68 |
| 15 | 27.89 | 1621 | −1770 | 310 | −137 |
| 20 | 32.29 | 1718 | −1852 | 698 | −196 |
| 25 | 39.72 | 2135 | −2005 | 1345 | −942 |
| 28 | 49.04 | 2171 | −2200 | 10911 | −9941 |
| 30 | 61.38 | 2225 | −2232 | 18099 | −11020 |
| 31 | 70.02 | 2263 | −2329 | 25839 | −17086 |
| 32 | 78.63 | 2291 | −2395 | 33915 | −20615 |
| 33 | 106.29 | 2457 | −2567 | 41278 | −35137 |

* At the mid-span of the beam. $\varepsilon_{et}$ is the maximum tensile elastic strain; $\varepsilon_{ec}$ is the maximum compressive elastic strain; $\varepsilon_{pt}$ is the maximum tensile plastic strain; and $\varepsilon_{pc}$ is the maximum compressive plastic strain

### 3.5 Parametric study

Many previous studies have shown that the charring rate of the wood component is related to its density closely. According to thermal response of wood illustrated in the European Standard EN 1991-1-2 (2003), the influence of the moisture content is only reflected in the small difference of wood density before the evaporation of water. Thus, the influence of the moisture content on the temperature field is very limited. In this study, finite element analysis (FEA) of the fire endurance takes the density and the load level as variable parameters.

3.5.1 Finite element models

Different densities set in FEA models are shown in Table 8. In Table 8, 100 denotes that the size of the component is 100×200×4000, and the value behind "-" is the density.

The establishment of the temperature field and the structure field FEA model, the prescribed load and boundary conditions, and the setting of solution options were given in Sections 3.4.1 and 3.4.2.

**Table 8 Densities set in FEA models**

| FEA model | Density (kg/m³) | Dry density (kg/m³) | Moisture content (%) |
|---|---|---|---|
| 100C37.5-450 | 450 | 389 | 15.8 |
| 100C37.5-600 | 600 | 518 | 15.8 |
| 100C37.5-750 | 750 | 648 | 15.8 |

3.5.2 Calculation results of the temperature field

Temperature variation at different depths of wood beams is shown in Fig. 13. Temperatures at different depths increase at different rates as the time in fire increases. The higher the density is, the slower the temperature increases. At the same time in fire, the smaller the density is, the higher the temperature at the same depth is.
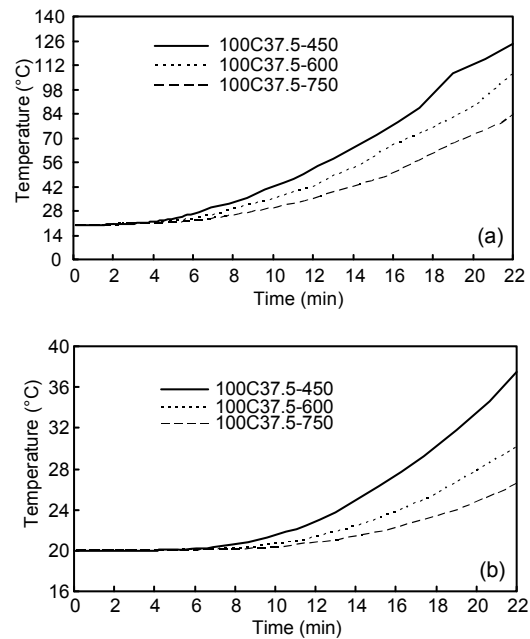


**Fig. 13 Temperatures at different depths changing with time in fire**
(a) 25 mm away from the edge of the beam; (b) 50 mm away from the edge of the beam

3.5.3 Calculation results of the structural field

Computation of displacements of models with different densities is shown in Fig. 14. In Fig. 14d, displacements are relative to the stage prior to fire with a specific load level.

As shown in Fig. 14, displacements at the mid-span of the beams with different densities increase as the time in fire increases and the ratio of increase becomes more rapid. Fire endurances of 100C37.5-450, 100C37.5-600 and 100C37.54-750 wood beams are 22 min, 25 min and 29 min, respectively. The higher the density is, the longer the fire endurance is, and the smaller the ultimate mid-span deflection is. The fire endurance increases about 32% as the density increases 67%.
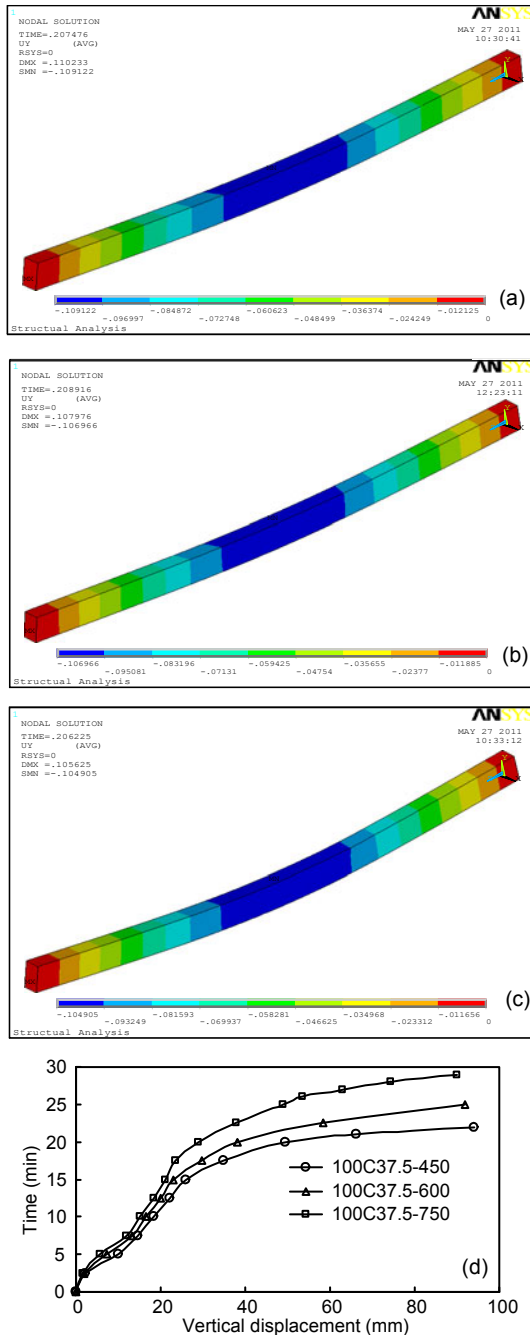
**Fig. 14 FEM calculation results of models with different densities (the unit is meter in Figs. 14a–14c)**
(a) Vertical ultimate displacements of the 100C37.5-450 beam; (b) Vertical ultimate displacements of the 100C37.5-600 beam; (c) Vertical ultimate displacements of the 100C37.5-750 beam; (d) Time-displacement curves

3.5.4 Relationships between fire endurances and load levels

Relationship between fire endurance and load level is shown in Fig. 15. Values of the horizontal coordinate were obtained through the non-dimensionalization method by taking the ultimate capacity of the contrast beam without fire as the reference point. As the load level increases, the fire endurance of the wood beam decreases and the reduction ratio become smaller. When the load level is greater than 0.5, the fire endurance is very small and it does not change significantly when the load level changes. When the load level is less than 0.5, the fire endurance maintains a linear relationship with the load level.
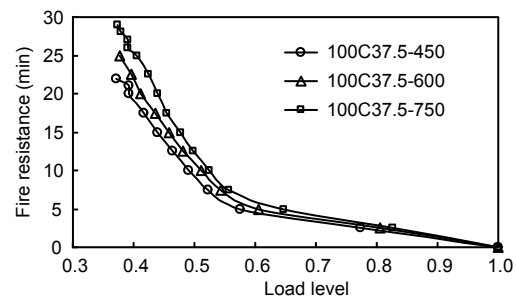


**Fig. 15 Relationships between fire endurances and load levels**

## 4 Conclusions

1. It has been shown from test results that the fire endurance of beams with the same cross section size decreases as the load level increases. When the load level increases from 25% to 37.5%, the fire endurance decreases from 28 min to 17 min. When the load level increases from 37.5% to 50%, the fire endurance decreases from 17 min to 13 min. The reduction ratio reduces as the load level increases. The fire endurance under the 50% load level increases 184% as the cross-section size increases 125%. Thus, the increase of cross section size is an efficient method to improve the fire endurance, and it can be improved about 38% by applying the fire protection coating.

2. In the process of the fire endurance test, the temperature of the test beam rises faster as the load level increases. The interior heating rate of the test beam with fire protection coating is obviously lower than that of the corresponding test beam without the fire protection coating in the early stage of the fire test.

3. From comparisons between FEM calculation results and test results of temperatures at 1#, 2#, 3# and 4# measure positions, it is found that calculation

results of 3# and 4# measure positions, 50 mm away from the edge, are matched perfectly with test values. Test values at 1# and 2# measure positions, 25 mm away from the edge, are greater than calculation results. The farther it is away from fire side, the closer FEM calculation results match test results. The predicted fire endurance is 33 min, and the experimental value is 28 min which is 18% smaller than the calculation one. The predicted ultimate mid-span deflection is 93 mm, and the experimental value is 117 mm which is 26% bigger than the calculation one. The discrepancy can be due to the fact that influences of structural field calculation results on the temperature field are not considered in FEM. But in actual test, defects of wood beams (such as cracks) accelerated the charring rate, which made the fire endurance reduced and made the mid-span deflection increased.

4. From FEM results, it is found that the mid-span deflection of the beams with different densities increases as the time in fire increases and the ratio of increase turns faster. Fire endurances of 100C37.5-450, 100C37.5-600 and 100C37.54-750 wood beams are 22 min, 25 min and 29 min, respectively. The fire endurance increases about 32% as the density increases 67%.

5. From FEM results, it can be seen that as the load level increases, the fire endurance of the wood beam decreases and the reduction ratio turns smaller. When the load level is greater than 0.5, the fire endurance is very small and it does not change significantly when the load level changes.

## References

Babrauskas, V., 2005. Charring rate of wood as a tool for fire investigations. *Fire Safety Journal*, **40**(6):528-554. [doi:10.1016/j.firesaf.2005.05.006]

Chen, X.J., Yang, L.Z., Deng, Z.H., Fan, W.C., 2002. A mathematical model for pyrolysis of wood in fire environment. *Journal of Combustion Science and Technology*, **8**(4):333-337 (in Chinese).

EN 1991-1-2, 2003. Eurocode 1: Actions on Structures. Part 1-2: Actions on Structures Exposed to Fire. Brussels, Belgium.

Firmanti, A., Subiyanto, B., Takino, S., Kawai, S., 2004. The critical stress in various stress levels of bending member on fire exposure for mechanical graded lumber. *Journal of Wood Science*, **50**(5):385-390. [doi:10.1007/s10086-003-0589-8]

Frangi, S.A., Bertocchi, M., Claub, S., Niemz, P., 2011. Mechanical behaviour of finger joints at elevated temperatures. *Wood Science and Technology*, in press. [doi:10.1007/s00226-011-0444-9]

Giancaspro, J., Papakonstantinou, C., Balaguru, P., 2009. Mechanical behavior of fire-resistant biocomposite. *Composites: Part B*, **40**(3):206-211. [doi:10.1016/j.compositesb.2008.11.008]

Hietaniemi, J., 2007. Probabilistic simulation of fire endurance of a wooden beam. *Structural Safety*, **29**(4):322-336. [doi:10.1016/j.strusafe.2006.07.016]

Hugi, E., Weber, R., 2012. Fire behaviour of tropical and European wood and fire resistance of fire doors made of this wood. *Fire Technology*, **48**(3):679-698. [doi:10.1007/s10694-010-0207-4]

ISO 834 (International Standards Organization), 1990. ISO/CD 834-1, ISO/CD 834-2 and ISO/CD 834-3, Fire Resistance Tests-Elements of Building Construction, Parts 1, 2, and 3.

Konig, J., 2005. Structural fire design according to Eurocode 5—design rules and their background. *Fire and Materials*, **29**(3):147-163. [doi:10.1002/fam.873]

Li, X.M., Li, S.X., Xu, Q.F., Xu, Q., Zhang, J., Mu, B.G., 2010. Experimental study on fire endurance of timber columns exposed to four-side fire. *Building Structure*, **40**(3):115-117 (in Chinese).

Lie, T.T., 1977. A method for assessing the fire resistance of laminated timber beams and columns. *Canadian Journal of Civil Engineering*, **4**(2):161-169. [doi:10.1139/i77-021]

Moss, P., Buchanan, A., Fragiacomo, M., Austruy, C., 2010. Experimental testing and analytical prediction of the behaviour of timber bolted connections subjected to fire. *Fire Technology*, **46**(1):129-148. [doi:10.1007/s10694-009-0096-6]

Njankouo, J.M., Detreppe, J.C., Franssen., J.M., 2005. Fire resistance of timbers from tropical countries and comparison of experimental charring rates with various models. *Construction and Building Materials*, **19**(5):376-386. [doi:10.1016/j.conbuildmat.2004.07.009]

Park, J.S., Lee, J.J., 2004. Fire resistance of light-framed wood floors exposed to real and standard fire. *Journal of Fire Sciences*, **22**(6):449-471. [doi:10.1177/0734904104042548]

Park, J.S., Buchanan, A.H., Lee, J.J., 2006. Fire performance of laminated veneer lumber (LVL) with glued-in steel rod connections. *Journal of Fire Sciences*, **24**(1):27-46. [doi:10.1177/0734904106053159]

Peng, L., Hadjisophocleous, G., Mehaffey, J., Mohammad, M., 2010. Fire resistance performance of unprotected wood-wood-wood and wood-steel-wood connections: A literature review and new data correlations. *Fire Safety Journal*, **45**(6-8):392-399. [doi:10.1016/j.firesaf.2010.08.003]

Pering, G.A., Springer, G.S., 1980. Decrease in tensile strength and in mass of burning wood. *Fire Technology*, **16**(4):245-251. [doi:10.1007/BF02473081]

Richardson, L.R., Batista, M., 2001. Fire resistance of timber decking for heavy timber construction. *Fire and Materials*, **25**(1):21-29.

Ru, H.W., Liu, W.Q., Lu, W.D., Yang, H.F., 2011. Fire resistance experiment on bolted connections in glued

laminated timber. *Journal of Nanjing University of Technology*, **33**(5):70-74 (in Chinese).

Van Zeeland, I.M., Salinas, J.J., Mehaffey, J.R., 2005. Compressive strength of lumber at high temperatures. *Fire and Materials*, **29**(2):71-90. [doi:10.1002/fam.871]

Xu, Q.F., Li, X.M., Mu, B.G., Zhang, J., Xu, M., Li, S.X., 2011a. Static experimental research on mechanical behavior of timber beams with lime putty finishing after fire. *Journal of Building Structures*, **32**(7):73-79 (in Chinese).

Xu, Q.F., Li, X.M., Zhang, J., Mu, B.G., Xu, Q., Li, S.X., 2011b. Experimental study of the mechanical behavior of timber beams exposed to three-side fire. *China Civil Engineering Journal*, **44**(7):64-70 (in Chinese).

Xu, Q.F., Li, X.M., Zhang, J., Mu, B.G., Xu, M., Li, S.X., 2012. Experimental study of the mechanical behavior of timber columns after exposure to fire on four sides. *China Civil Engineering Journal*, **45**(3):79-85 (in Chinese).

Yao, L.H., Wang, X.M., Fei, B.H., Zhao, R.J., 2007. Present status of fireproofing for wooden buildings. *China Wood Industry*, **21**(5):29-31 (in Chinese).

Ye, X.L., Shi, Y.J., 2003. Application Examples of Engineering Analysis Software—ANSYS. Tsinghua University Press, Beijing, China (in Chinese).

Young, S., Clancy, P., 2001. Compression mechanical properties of wood at temperatures simulating fire conditions. *Fire and Materials*, **25**(3):83-93. [doi:10.1002/fam.759]

## Welcome Your Contributions to *JZUS-C*

*Journal of Zhejiang University-SCIENCE C (Computers & Electronics)*, split from *Journal of Zhejiang University-SCIENCE A*, covers research in Computer Science, Electrical and Electronic Engineering, Information Sciences, Automation, Control, Telecommunications, as well as Applied Mathematics related to Computer Science. *JZUS-C* has been accepted by Science Citation Index-Expanded (SCI-E), Ei Compendex, DBLP, IC, Scopus, JST, CSA, etc. Warmly and sincerely welcome scientists all over the world to contribute Reviews, Articles, Science Letters, Reports, Technical Notes, Communications, and Commentaries.